Impedance Measurements of Motor Drive and Supply in SPEED Testbed

Timothy P. Dever*, Xavier Collazo†, Patrick Hanlon†, Keith R. Hunker*, David J. Sadey†, Casey Theman‡, Brian P. Malone†
NASA Glenn Research Center, Cleveland, OH, 44135

Many electrified aircraft configurations consist of a number of power components operating on the same shared electrical bus. Understanding the impedance performance of electrical loads and sources is key to understanding, and designing for, acceptable overall vehicle power quality and power system stability. To enable these measurements, personnel at NASA's Glenn Research Center have designed and built the Scaled Power ElEctrified Drivetrain (SPEED) Testbed. This paper will present data taken in the SPEED lab, including impedance measurements of a DC supply (source) and a motor drive and electric machine (load) under a number of conditions. Impacts of load power, drive controller tuning, and field-weakening on load impedance are measured, presented, and discussed; as are source impedance data, stability, and DC bus current spectra at different loading levels.

I. Nomenclature

AREAL	=	Advanced Reconfigurable Electrified Aircraft Laboratory
EPS	=	Electrical Power System
EAP	=	Electrified Aircraft Propulsion
HVDC	=	High Voltage Direct Current
IMS	=	Impedance Measurement System
NASA	=	National Aeronautics and Space Administration
PQ	=	Power Quality
RVLT	=	Revolutionary Vertical Lift Technology
SPEED	=	Scaled Power ElEctrified Drivetrain
Z	=	Impedance

II. Introduction

The Scaled Power ElEctrified Drivetrain (SPEED) Testbed, located at NASA Glenn Research Center (GRC), is intended for development of power system measurement techniques [1]. SPEED is a low power testbed intended to complement the Advanced Reconfigurable Electrified Aircraft Laboratory (AREAL), a 200 kW High Voltage DC (HVDC) lab, also located at NASA GRC, which will be used to test various electric power system (EPS) architectures and utilization equipment [2]. Both SPEED and AREAL include DC supplies, drives, and electric machines for testing purposes.

This paper will describe setup of, and present results from, source and load impedance measurements; the load being a motor drive and electric machine combination in motoring mode, and the source being a DC supply. These were the first measurements of this type performed at NASA GRC. The goal of these measurements is to understand the impedance performance of electrical loads and sources. These measurements are intended to assist with the understanding of, and designing for, acceptable overall Electrified Aircraft Propulsion (EAP) vehicle power quality and power system stability.

* Electrical Engineer, Diagnostics and Electromagnetics Branch, 21000 Brookpark Rd MS 309-2.
† Electrical Engineer, Power Management and Distribution Branch, 21000 Brookpark Rd MS 301-5.
‡ Electrical Engineer, Space Power and Propulsion Test Engineering Branch, 21000 Brookpark Rd MS 333-1.

Section III of this paper provides an overview of the SPEED testbed and details of its relevant components. Additionally, a description of the impedance measurement approach and the test configuration is presented. In Section IV, load (machine/drive) impedance measurements and results are covered. First, selection of the testing conditions is discussed; then measurement data is presented, covering the impact on load impedance of load power (machine speed and torque test points spanning the allowed range of operation); next, drive controller tuning is presented, followed by field-weakening. In Section V, source (DC supply) impedance results are presented and discussed, as are system stability, and current spectra measured on the DC bus under various loading conditions. This paper is a companion to [3], which discusses impedance testing in NASA's Electric Aircraft Testbed (NEAT).

III. SPEED Testbed Overview

A schematic of the SPEED Testbed configuration during testing is shown in Fig. 1. A photo of the lab is included in Fig. 2. The SPEED Lab consists of a DC supply, a commercial-off-the-shelf (COTS) permanent magnet synchronous motor (PMSM), a motor drive (and controller, not shown); a hysteresis dynamometer ('Dyno'); and a cooling system (not shown).

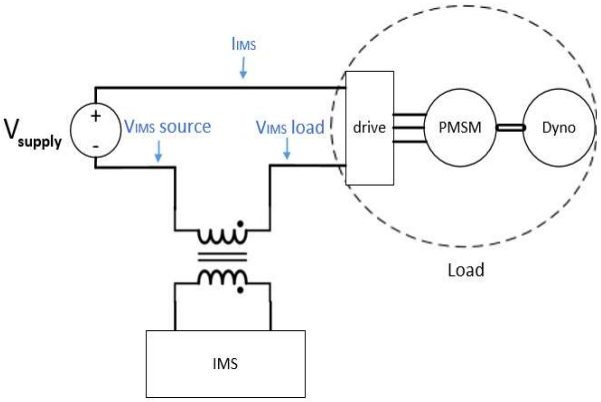

Fig. 1 Schematic of SPEED lab

For this impedance testing, an Impedance Measurement System (IMS) was added. The IMS consists of a control computer and a Frequency Response Analyzer. The IMS generates low level sinusoidal test signals swept over the desired frequency range, and includes a power amplifier to amplify these signals; as well as analog inputs, and software which performs the impedance calculations. A transformer is used to inject the signals from the power amplifier. Voltage and current measurements are taken to provide input measurements for impedance calculations. During testing, both load and source impedances were measured. Current measurements (I_{IMS}) were common to both impedance load and source measurements; source voltage ($V_{IMS\ source}$) was measured on the source side of the transformer, and load voltage ($V_{IMS\ load}$) was measured on the load side of the transformer. Impedance measurements were performed by injecting and sweeping a test signal, measuring voltage and current at specific frequencies, and using those measurements to calculate load and source impedances at those frequencies. In a separate set of tests, current spectra were calculated by capturing DC current at I_{IMS} via a high-speed oscilloscope under various system conditions, and post-processing the measurement data to generate the desired spectra.

The DC supply was capable of providing sufficient power for all test points, and was run at several voltages during testing (300 Vdc maximum). The peak output power of the motor drive was 100 kVA, and the rated power of the PMSM was 14 kW; however, the dyno was limited to 6 kW continuous, and 7 kW peak (under 5 minutes), and was thus the pacing component for testing. A summary of system component ratings is included in Table 1.

Table 1 SPEED Component Ratings

Component	Rating
Motor Rated Output power	14 kW
Inverter Peak output power	100 kVA
Dyno Power Rating	7 kW (5 minutes) 6 kW (continuous)

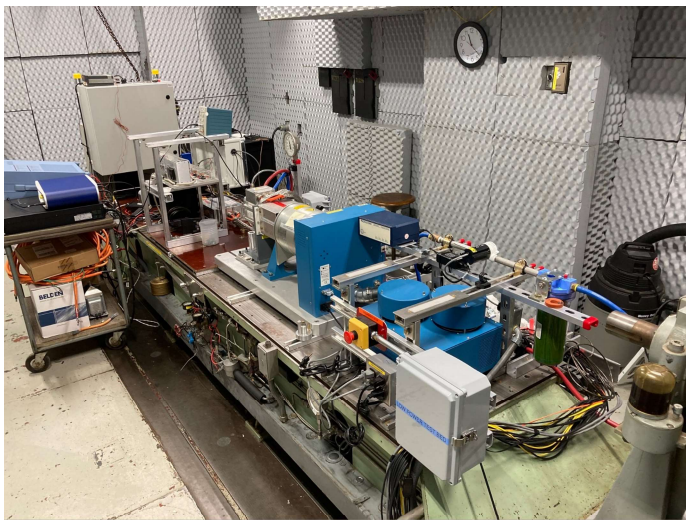

Fig. 2 Photo of SPEED Lab

IV. Load Impedance Tests

This section covers the load impedance testing, i.e., the testing of the motor drive and the PMSM, loaded by the dyno. Topics covered include a discussion of the selected load impedance test conditions and test points, and the impacts on load impedance due to load power changes, drive controller tuning, and to entering the field-weakening regime.

A. Test Conditions and Point Selection

Test points were selected by choosing test conditions which enabled safe operation within the SPEED lab. This discussion can be naturally divided into two topics: safe facility operation, and safe IMS operation.

The approach to safe facility operation was to first understand, then bound, safe SPEED lab power component operating conditions. As discussed in the previous section, the PMSM and motor drive were capable of higher power operation than that of the dyno, making the dyno the pacing element. Accordingly, test points (PMSM speed and dyno applied torque) were selected to ensure that the machine power achieved remained beneath the dyno maximum. The selected load impedance measurement test points are shown in Fig. 3. Note that numerous motor speeds and torque loading levels were explored. Also note that the corner, which is the highest torque (10 Nm) and highest speed (8000 rpm) condition, was avoided, as this test point exceeded the dyno power limit of 7 kW.

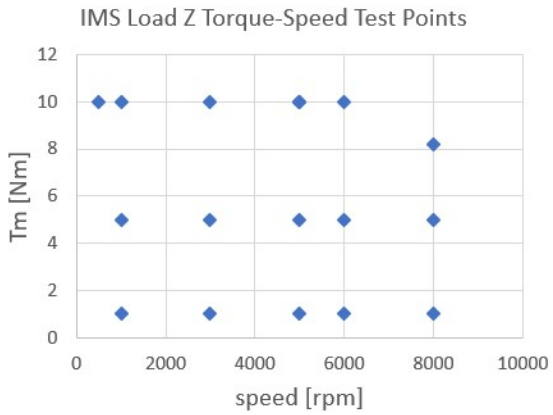

Fig. 3 Load Impedance Test Points

Safe IMS operation required several considerations: setting frequency limits, transformer temperature monitoring, and defining injected signal level. IMS frequency testing limits were defined before testing began. They were set to 30 Hz as a minimum, and 100 kHz as maximum. These were set based on limits provided by the transformer datasheet. Transformer health was observed by attaching a thermocouple to the transformer and continuously monitoring temperature. Temperature rise was minimal throughout testing, and so the transformer was kept well within its power limits.

One approach to performing impedance measurements on power loads is to select a single injected signal voltage level and maintain it throughout the entire testing frequency range. As this was the team's first impedance measurement of a motor/drive combination, a more cautious approach was deemed necessary. A large variation in impedance was considered a possibility with this system, which would result in extremely large injected currents at low-impedance frequencies; so a trial-and-error method was adopted, and levels were determined by experiment. With the motor/drive/dyno operating at a low speed and torque, the injected signal was swept through the frequency test range while the resultant injected current on the DC link was monitored. The injected signal was at first set to a very low level and gradually increased to ensure that the resultant current signal was maintained at a reasonable level throughout: i.e., small enough to allow small-signal levels as desired, but large enough to enable non-noisy impedance measurements.

This approach resulted in division of the load impedance measurements into two regions, and adoption of a dual level signal injection scheme, as listed in Table 2. A larger injected voltage signal was used in the low frequencies (30 to 1000 Hz); and a smaller signal was used at high frequencies (between 1 and 100 kHz). It should be noted that the conservative approach was shown to be appropriate. As will be discussed in the next section, the measured load impedance was observed to vary over three orders of magnitude across the frequencies tested. Use of injection signal magnitudes appropriate for low frequency measurements across the entire frequency range would have resulted in dangerously high currents in the low impedance region; therefore, the dual sweep approach was warranted with this system.

Table 2 Load Measurement

Load Sweep Definition			
sweep	**Fstart**	**Fend**	**signal**
LF	30	1100	1
HF	900	100k	0.05

B. Load Power Impact on Load Impedance

Load impedance measurements were performed for all of the test points listed in Fig. 3, using the load sweep definitions described in Table 2. Results are shown in Fig. 4.

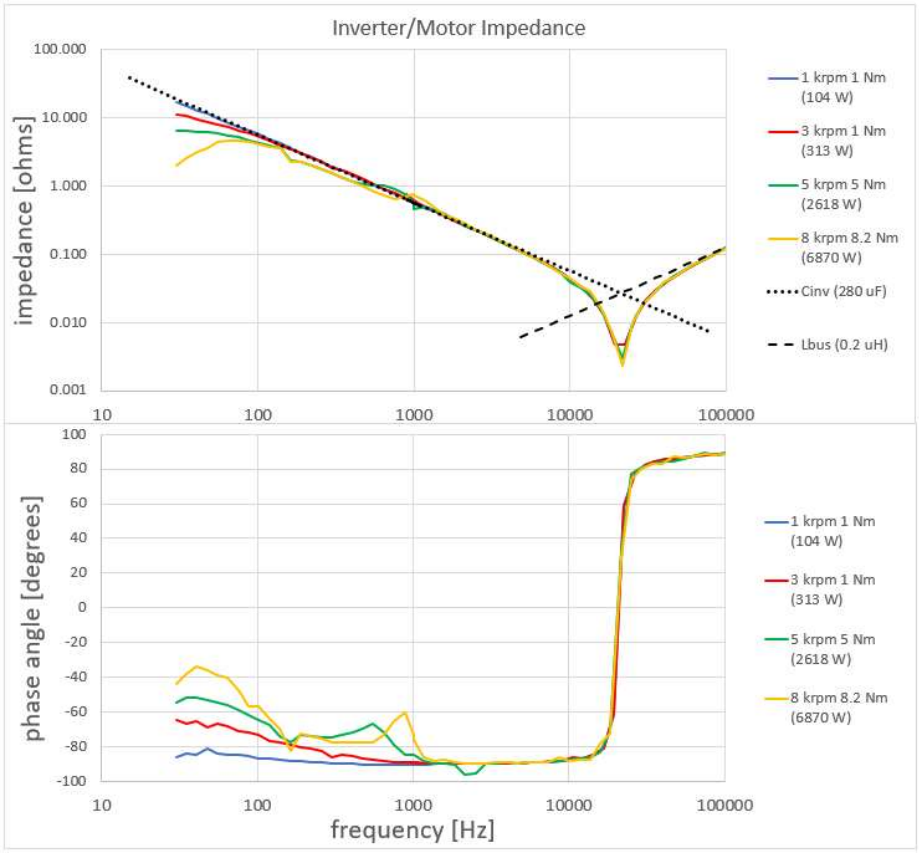

Fig. 4 Load Impedance at Varying Motor Operating Points

There was much similarity in the measured load impedance throughout the defined test range. In fact, under all test conditions, impedance behavior varied very little in frequencies exceeding 3 kHz. In Fig. 4, representative load impedance data was selected to display the overall commonality, and to illustrate observed trends where changed behavior was observed.

One interesting observation is the variation in load impedance magnitude over the tested range. At 100 Hz, load impedance under all test conditions was about 5 Ω; while at the impedance minimum (about 22 kHz), the load impedance was only 3 mΩ - a three order of magnitude difference.

The structure of the load impedances was very similar under the different test conditions. At lower frequencies, the impedance looked capacitive. This appears to be defined by the input filter capacitor of the motor drive, which, according to the datasheet, has a value of 280 uF (also plotted in Fig. 4, top); note the measured impedance matches this value very closely between 100 Hz and 10 kHz, and that the phase angle in this region is -90°, as expected. At higher frequencies, the load impedance appears inductive; the phase angle nears +90°, and the magnitude appears to asymptote to about 0.2 uH (also plotted). Note that the resonance point is in the same location for all measurements, near 22 kHz.

Load impedance variation as a function of delivered power was observed. For example, at the lowest measured frequency, we see decreased load impedance magnitude with increased power delivered; this is expected with a drive/machine system, as it constitutes a constant power load [4]. We also expect the phase angle to move to -180° at lower frequencies in a constant power load, which was not observed. The assumption is that this would be observed with measurements taken at low enough frequencies; note that this low frequency measurement capability is presently being developed [2], and that anticipated future testing will prove this out.

One interesting and unexpected feature occurs in the phase data below 1 kHz. As mentioned above, this phase angle is expected to eventually decrease to -180°; but in this region, the phase angle actually increases in value with increased delivered power; up to nearly -30° for the highest power case (6870 W, near the dyno max of 7 kw peak) before beginning to decrease again. This warrants further study, and may possibly have stability impacts, depending on the impedance characteristics of the selected source.

Note that the structure of the drive/machine impedance is consistent with that predicted for a similar load in [5].

C. Drive Controller Tuning Impact on Impedance

In this section, two of the tuning parameters in the motor drive were modified, and tuning impact on load impedance was measured.

Numerous tuning parameters were available within the drive controller. As test time was limited, not all could be checked; the two gains selected for test were the proportional gain (Kp) and integral gain (Ki) within the current loop. They were chosen because simulation predicted that these gains would have the largest impact on performance. Sets of gain pairs were chosen to vary over a large range; a map of the selected tuning test points is shown in Fig. 5, with the nominal tuning (Kp = 2000, Ki = 100) circled in red. Additionally, a consistent motor torque and speed setting was chosen, and a 1000 rpm and 5 Nm operating point was run for all test points.

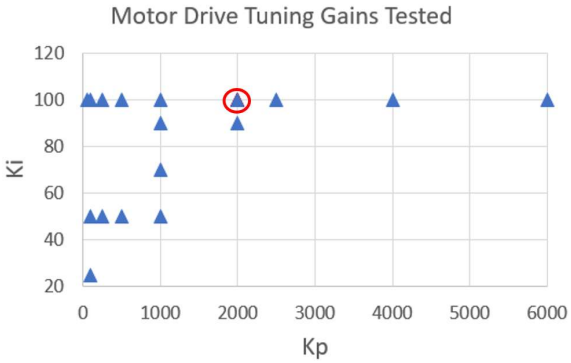

Fig. 5 Tuning Test Points

To perform the test, the tuning gains were programmed into the drive; the drive/motor/dyno was operated at the selected speed and torque test point; the IMS sweep was run; voltages and currents were measured; and the load impedance was calculated. This process was repeated for all of the points shown in Fig. 5.

The measured impedance data is displayed in Fig. 6, for all 17 data points listed in Fig. 5. Note that there is significant relevant tuning impact at lower frequencies, below about 500 Hz. Since nothing of interest was observed at higher frequencies, only a single, representative high frequency impedance trace is shown.

While operating at the selected speed and torque conditions, increases in Kp and Ki both tended to drive load impedance magnitude and phase toward capacitive behavior: magnitude toward the -20 dB/decade line, and phase angle toward -90°. There are numerous variables in play; one example result is provided, for Kp impact on phase angle, while Ki (and motor torque and speed) is held constant, as shown in Fig. 7. Note that as Kp increases, the phase angle in this frequency range moves closer to -90°.

Note that this is not an exhaustive tuning study. Firstly, as with all measurements reported in this paper, impacts to impedance beyond the measured

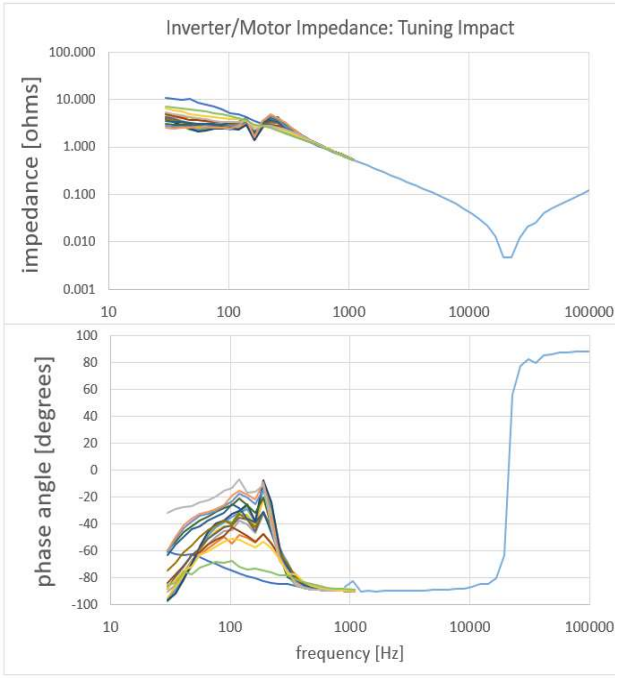

Fig. 6 Tuning Impact on Load Impedance

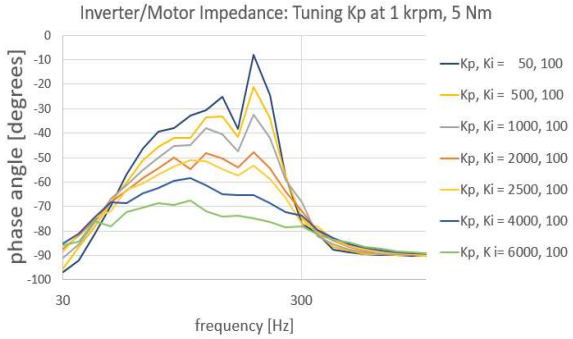

Fig. 7 Tuning Impact: Kp on Load Phase Angle

frequencies might be relevant. Additionally, this test was performed at one single motor power (speed and torque) point; behavior at other motor test points may vary. Also, there are numerous other tuning parameters to consider; e.g. speed loop gains, field-weakening gains, etc. It is intended that these investigations will be performed in future work. However, despite the above-described limitations, these measurements do indicate that, within the observed frequency range and with this setup, low frequency impedance shaping via motor drive controller tuning is possible.

D. Field-Weakening Impact on Load Impedance

In this section, the impact on load (drive/PMSM) impedance behavior when the motor drive enters field-weakening control was investigated. The goal was to check load impedance under multiple conditions: during drive operation in the standard (constant torque) region, and then at several points as the drive was sent further and further into the field-weakening control (constant power) region.

One possible approach to setting up these operating conditions would be to maintain DC bus voltage, set torque on the dyno, and increase commanded motor speed until the field-weakening regime was entered. This was considered unattractive for several reasons. Firstly, this approach could potentially exceed the dyno power rating; and secondly, motor speed would be changing with each test point. Instead, a simple approach which would ensure safe dyno operating conditions and maintain motor operating conditions was implemented. First, a constant motor operating point was selected, which held delivered mechanical power, machine speed (6 krpm) and delivered torque (5 Nm), constant throughout testing. Next, the DC bus voltage (DC input to motor drive) was decreased in steps, and drive/machine impedance was tested at multiple points. Measurement results are shown in Fig. 8.

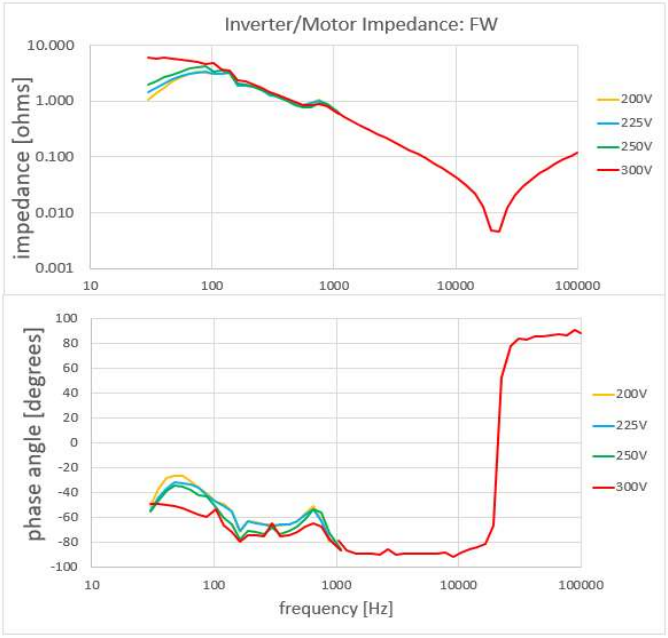

Fig. 8 Field-Weakening Impact on Load Impedance

Fig. 8 shows measured load impedance at four DC motor drive input voltages. By monitoring drive feedback parameters (modulation index and d-axis current), it was determined that when operating at the first test point (Vsource = 300 V) the drive was in constant torque mode; and while at the other three points (Vsource = 250, 225, and 200 V) the drive was in field-weakening mode.

Results show that entry into the field-weakening mode impacted the impedance magnitude and phase in the lower frequency range (under 1 kHz). With increased field-weakening, impedance magnitude decreased, while the phase angle moved away from pure capacitive (-90°). Based on the results of the previous sections, the effects of increased field-weakening were similar to those of increased machine loading; and of decreased current loop tuning gains (Kp and Ki). Dynamic transitions into the field-weakening regime could be considered for future source-load stability assessments.

V. Source Measurement Results

This section covers measurements performed on the DC supply. Source impedance measurement and bus current spectrum data are presented and discussed.

A. Source Impedance Data

Before taking any impedance measurements of the source, the injected signal magnitude was selected by experiment, using the same process as that described in Section IV-A. A trial signal level was used at first, at a very low level, and gradually increased to ensure that the injected current signal maintained a reasonable level through the test frequency band. This process again resulted in a two-level injection scheme, but the identified breakpoint was changed, moving from the 1 kHz used for load measurements, down to 175 Hz for the source measurements (see Table 3). Note that during testing, signals are injected on both the load and source side; thus this selection was attractive, as it avoided injection of large signals in the low impedance region of the load (around 22 kHz, per Fig. 4).

Table 3 Source Measurement

Source Sweep Definition			
sweep	**Fstart**	**Fend**	**signal**
LF	30	200	1
HF	150	100k	0.05

As with the load measurements, there was much commonality in the source impedance measurements under different loading conditions, particularly at higher frequencies. Results of representative source impedance measurements are shown in Fig. 9.

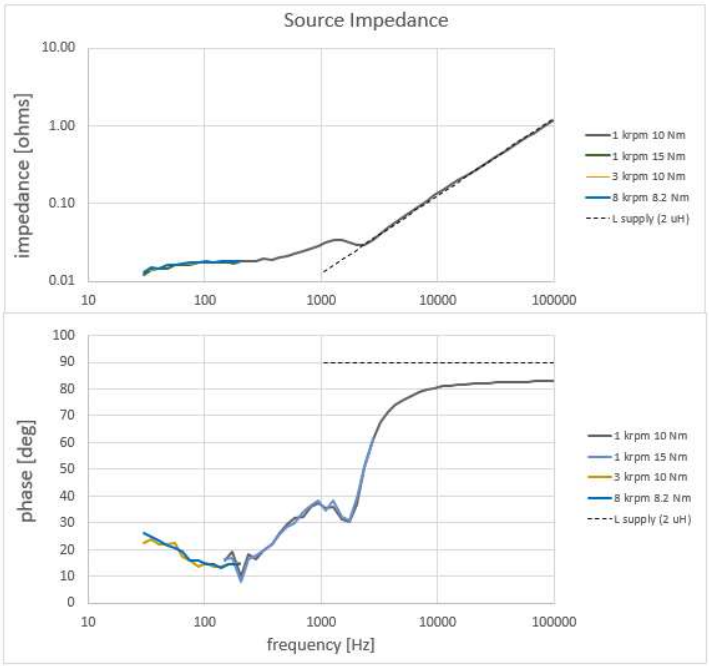

Fig. 9 Measured Source Impedance

As seen in Fig. 9, the source approaches inductive behavior at higher frequencies (above ~ 5 kHz): magnitude increasing at the rate of 20 dB/decade, and phase angle approaching +90°. It is assumed that the inductance measured is dominated by that of the source (rather than the fairly short lead cables); an assumed supply inductance of 2 uH is plotted along with the data. Note that the high frequency behavior is similar to that seen in the load impedance, although there are some obvious differences, e.g. the source impedance inductance value is 10x higher, and the break point frequency is lower. Unlike with the load impedance, at lower frequencies the supply acts more resistive than capacitive; flat impedance magnitude, and phase angle closer to zero than to -90°.

B. Stability Assessment

While stability performance was not a requirement during the original design effort for the SPEED lab, the stability of the system was worth quantifying. Since both source and load impedance was available, an assessment, within the frequency range studied, was straightforward.

To assist in this effort, source impedance (Z_S) and load impedance (Z_L) were plotted together, in Fig. 10. Next, arbitrary stability margins of 6 dB and 45° were selected, and a Nyquist plot of Z_S/Z_L was made; shown in Fig. 11.

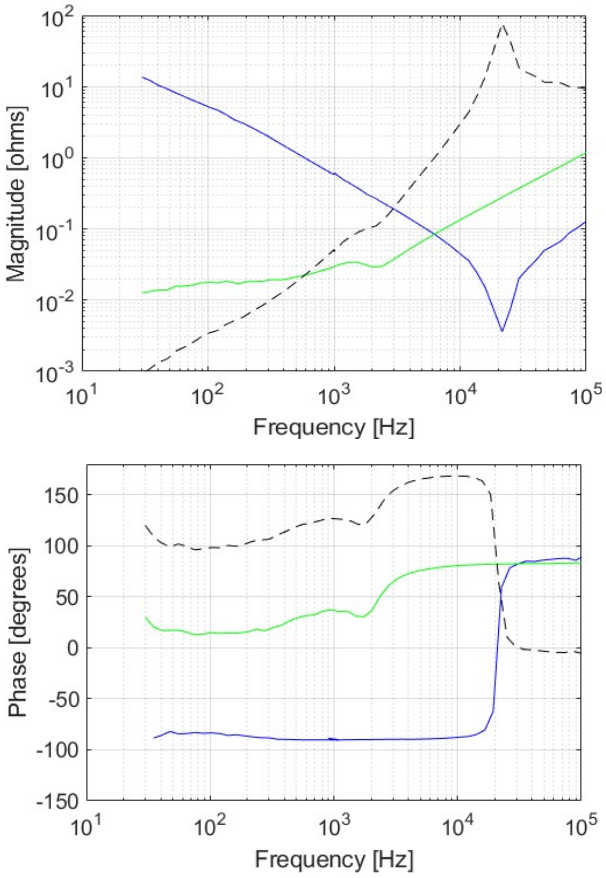

Fig. 10 Measured source Z (green) & load Z (blue); Dashed: top, $|Z_S/Z_L|$; bottom, phase angle difference

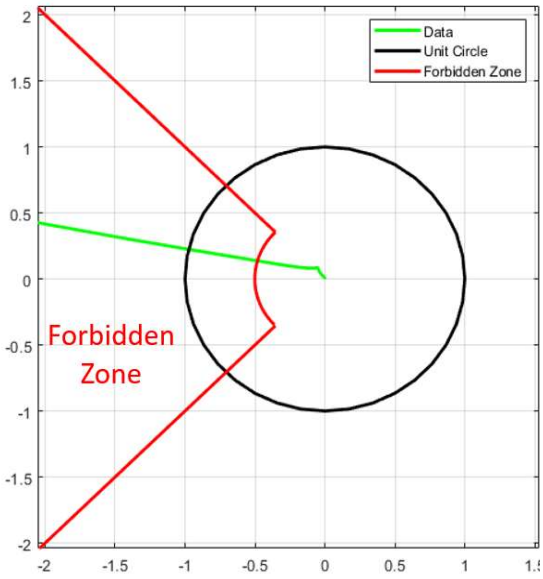

Fig. 11 Z_S/Z_L Nyquist plot

In Fig. 10 (top), magnitudes of Z_S and Z_L are plotted, along with $|Z_S/Z_L|$ (dashed line). In Fig 10. (bottom), phase angles of the impedances are shown, along with their differences (source Z phase angle - load Z phase angle, dashed line). These plots, in the frequency range measured (30 Hz to 100 kHz), demonstrate a phase margin of 11 degrees. The corresponding Nyquist plot of Z_S/Z_L, in Fig. 11, shows that the arbitrary margins are not met, as expected. Much of the plot is off scale, as expected given the large magnitude of the ratio (approaching 100, per Fig. 10, top).

SPEED system has been very successful in terms of enabling testing. However, while this narrow stability margin did not impact performance in the SPEED lab, this analysis does point out potential areas of improvement (e.g. adding filtering) in future work.

C. Bus Current Spectra

The spectrum of the DC bus current was studied under varied machine loading conditions. This topic was of interest, to gain an understanding of potential forcing frequencies injected on the bus.

This testing was done under numerous loading conditions: at four machine speeds (1, 3, 6, and 8 krpm) and three torque levels (0, 5, and 10 Nm). Current spectra were calculated by capturing measured DC current (I_{IMS}, see Fig. 1) on a high-speed oscilloscope, and post-processing the data to generate spectral plots. The results can be best discussed by dividing them into two categories: low frequency results, and higher frequency results (centered around the drive switching frequency). Representative data is displayed in Fig. 12 and Fig. 13.

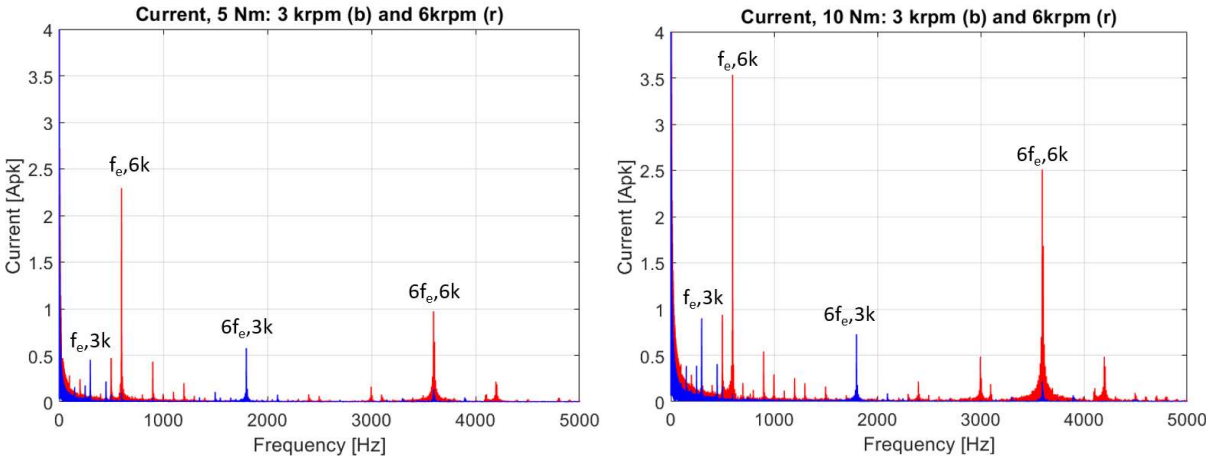

Fig. 12 Example Bus Current Spectra Results, low frequency

Two sets of low frequency spectra are included in Fig. 12: plots for two speeds (3 and 6 krpm), shown on both plots; and machine loadings of 5 Nm (left plot) and 10 Nm. The dominant current peaks are the electrical speed, f_e, and six times electrical, or $6f_e$ (which is also the mechanical speed, as the PMSMs are 12 pole machines). Note that the magnitudes of the current peaks increase with increased speed (seen in both plots); and with increased load torque (seen when comparing plots).

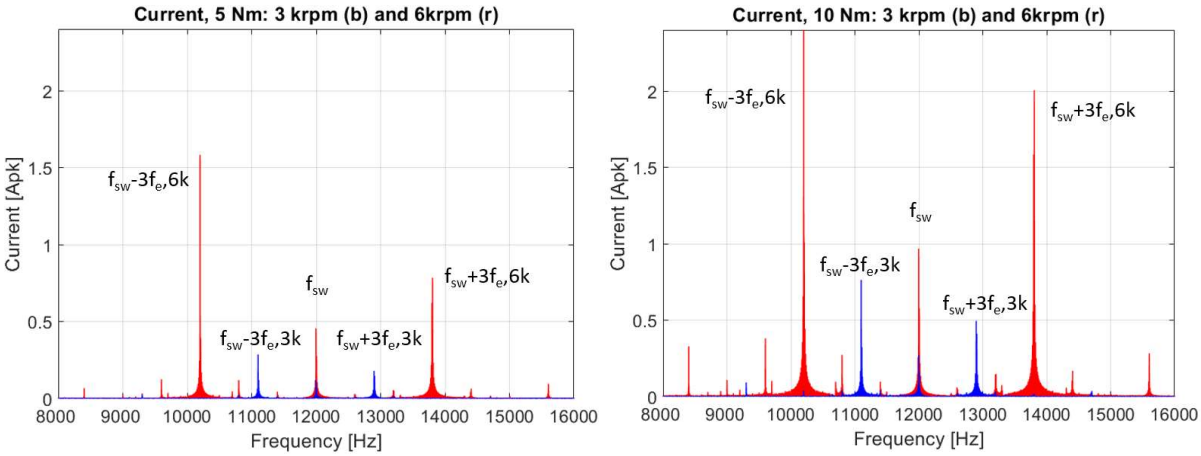

Fig. 13 Bus Current Spectra Results, centered at switch frequency

Two sets of high frequency spectra, centered at the motor drive switching frequency, are included in Fig. 13. Again, plots for two speeds (3 and 6 krpm) are shown in both plots; and machine loadings vary from 5 Nm (left plot) to 10 Nm.

Note that the measured switch frequency matches the frequency described in the motor drive specification (12 kHz), marked as f_{SW}. The dominant peaks in the measured data in all cases occurred in the same three places: at the switch frequency, and at switch frequency plus and minus three times the electrical frequency ($f_{SW} \pm 3f_e$). As with the

low frequency data, current peak magnitude increases with speed (as seen in data pairs in both plots), and with increased loading (comparing left to right plots).

VI. Conclusions and Future Work

This paper presents source and load impedance measurements in the NASA GRC SPEED Lab. The source tested was a DC supply, and the load test was a motor drive, driving a PMSM which is loaded with a dynamometer. An overview of the SPEED lab components and the measurement equipment and test procedure is first provided. Next, load impedance measurements and results are presented and discussed, including impacts on load impedance from machine speed and torque, drive controller tuning, and drive entrance into the field-weakening control regime. Finally, source impedance results, system stability, and DC bus current spectra under various loading conditions are presented and discussed.

These are the first measurements of their kind performed at NASA GRC. Potential future work includes testing at lower frequencies and at higher power; further investigation into drive tuning impacts (additional tuning parameters, wider range of study) on load impedance behavior; load susceptibility to bus ripple; input filtering additions and impacts with the inverter/motor pair; stability implications due to source/load interactions within a high power HVDC system; and field-weakening impacts to system stability.

Acknowledgments

The authors would like to thank the Revolutionary Vertical Lift Technology (RVLT) Project, the Electrified Powertrain Flight Demonstration (EPFD) Project, and the Advanced Air Transport Technology (AATT) Project for supporting this work.

References

[1] Hanlon et al., “NASA Scaled Power ElEctrified Drivetrain”, 2023 AIAA/IEEE Electric Aircraft Technologies Symposium (EATS).

[2] Sadey, David J. et. al., “NASA Advanced Reconfigurable Electrified Aircraft Laboratory (AREAL)”, 2023 AIAA/IEEE Electric Aircraft Technologies Symposium (EATS).

[3] Dever, Timothy P. et al., “Impedance Measurements of Motor Drives and Supplies in NASA NEAT Facility”, 2023 AIAA/IEEE Electric Aircraft Technologies Symposium (EATS)

[4] Kascak, Peter, Timothy Dever, and Ralph H. Jansen. "Electric Aircraft Propulsion Power System Impedance Modelling Methodology." 2021 AIAA/IEEE Electric Aircraft Technologies Symposium (EATS). IEEE, 2021.

[5] Dever, Timothy P., Peter E. Kascak, and Ralph H. Jansen. "Megawatt Electric Aircraft Propulsion Power System Impedance Modelling." 2022 IEEE Transportation Electrification Conference & Expo (ITEC). IEEE, 2022.